JOC The Journal of Organic Chemistry

Article

Tautomerism-induced Cis-Trans Isomerization of Pyridylethenyl N-Confused Porphyrin

Ryuichi Sakashita, Yasutaka Oka, Hisanori Akimaru, Praseetha E. Kesavan, Masatoshi Ishida, Motoki Toganoh, Tomoya Ishizuka, Shigeki Mori, and Hiroyuki Furuta

J. Org. Chem., **Just Accepted Manuscript** • DOI: 10.1021/acs.joc.7b01770 • Publication Date (Web): 26 Jul 2017

ACS Publications

The Journal of Organic Chemistry is published by the American Chemical Society. 1155 Sixteenth Street N.W., Washington, DC 20036

Tautomerism-induced *Cis-Trans* Isomerization of Pyridylethenyl N-Confused Porphyrin

Ryuichi Sakashita,[†] Yasutaka Oka,[†] Hisanori Akimaru,[†] Praseetha E. Kesavan,[†] Masatoshi Ishida,[†] Motoki Toganoh,[†] Tomoya Ishizuka,[‡] Shigeki Mori,[§] and Hiroyuki Furuta*[†]

[†]Department of Chemistry and Biochemistry, Graduate School of Engineering, Kyushu University, Fukuoka 819-0395, Japan

[‡]Department of Chemistry, Faculty of Pure and Applied Sciences, University of Tsukuba, Tsukuba 305-8571, Japan

[§]Advanced Research Support Center, Ehime University, Matsuyama 790-8577, Japan

ABSTRACT: Pyridylethenyl-substituted N-confused porphyrins (NCPs) were synthesized and their *cis-trans* isomerization was studied. Among 4 possible isomers, *trans*-3H and *cis*-2H types of structures, of which aromaticity and absorption/emission properties differ largely, were isolated. The *cis*-isomer was largely stabilized by the intramolecular hydrogen bonding between the pyrrolic-NH and the pyridinic-N in the vicinity. The thermal *cis-trans* isomerization proceeded even at 30 °C, which was significantly accelerated by the pyridine added to the system. The kinetic studies revealed the isomerization reaction was second order and the activation energy of the thermal isomerization from *cis* to *trans* isomer was $\Delta G_o^{\ddagger}{}_{cis\rightarrow trans}$ = 35.7 kcal/mol at 298 K, which is significantly smaller than that of Ni complex, 42.3 kcal/mol. Intermolecular proton transfer induced *cis-trans* isomerization mechanism was proposed.

INTRODUCTION

A set of interconvertible isomers, of which structures and electronic properties differ largely, is an attractive candidate for the applications such as optical memories and switches at the molecular level.[1] A variety of isomerization systems, such as *cis-trans* azobenzenes, ring *open-closed* diarylethenes, *keto-enol* tautomers, etc., have been so far developed for such purpose.[2] Among them, the usage of *cis-trans* isomerization of simple diarylethene is rather limited compared with that of azo systems because of the smaller difference in the optical properties between the *cis-trans* pair and succeeding ring-forming reactions. If one of the isomers largely alters its electronic state through a specific interaction between the aryl groups at both ends, a distinct difference could be anticipated. One of the strategies to cause such a change is to make the two aryl groups bifunctional and interactive each other in the *cis*-form. (Schemes 1a). The acid-base pair could be anticipated as a candidate for the aryl groups, and actually, an olefin molecule with a pyrrole-pyridine substituent-pair, 2-[2-(2-pyrrolyl)ethenyl]pyridine (**Py-C=C-Pyr**), was reported to show a distinct difference in the fluorescence spectra; *cis*: λ_{max} = 570 nm and *trans*: λ_{max} = 430 nm (Schemes 1b).[3]

Meanwhile, we have been working on the N-confused porphyrin (NCP) since its discovery.[4] NCP can take two NH tautomeric forms, inner 3H- and inner 2H-form, electronic states of which are totally different.[5] Namely, the 3H-tautomer, which possesses three protons inner core (2NH, 1CH) as well as an imino-type N at the periphery, exhibits a strong aromaticity due to the complete annulenic circuit in the porphyrin skeleton. On the other hand, 2H-tautomer possesses only two inner protons (1NH, 1CH) and an amino-type outer NH, annulenic circuit of which is incomplete. As the result, the two tautomers show the electronic properties with marked difference.[5] These tautomers interconvert easily and this NH tautomerism can be controlled by the external molecules such as solvents[5] or anions[6], and each tautomeric form can be fixed by metalation (e.g., Co^{II},[7a] Ni^{II},[4b] Cu^{II},[7b] Pd^{II},[7c] Pt^{II},[7d] for 2H-form and Co^{III},[7e] Cu^{III},[7f] Ag^{III} [7g] for 3H-form).[8]

Scheme 1. *Cis-Trans* Isomerization of Alkene with Interacting groups: a) Conceptual Illustration, b) Py-C=C-Pyr, and c) Pyridylethenyl NCP

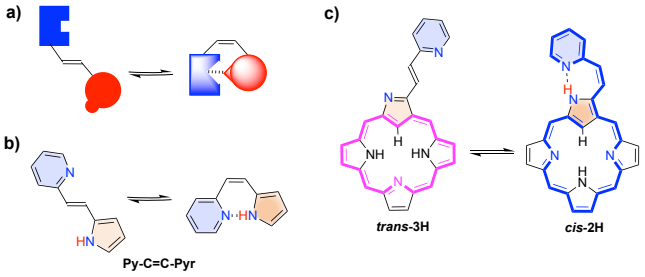

From the structural point of view, NCPs can be regarded as *expanded pyridine* and/or *expanded pyrrole* (and *expanded imidazole* in the case of doubly N-confused porphyrins) according to the tautomeric forms, because an outward-pointing nitrogen atom exists at the periphery of a large conjugated macrocycle.[9] In fact, we have already demonstrated the pyrrole-like anion binding,[6,10] pyridine-like metal coordination,[11] and imidazole-like acid-base interactions with NCPs.[12] Thus, we could develop a Gulliver-type pyridine/pyrrole chemistry by utilizing NCPs to enlarge the functionality. Here, the idea is to expand the 6π-based isomerization system to the 18π NCP-based one by simply changing the aryl groups. In this study, we synthesized pyridylethenyl-NCP (**1**), in which a

pyrrole moiety of **Py-C=C-Pyr** was replaced with NCP. The regular porphyrin derivative (**7**) was also synthesized for a reference (Scheme 2). We found the colors of the solutions of two isomers, ***cis*-2H-1** and ***trans*-3H-1**, were largely different and the *trans* isomer showed the intense emission. Surprisingly, the *cis-trans* thermal isomerization of **1** proceeded even at 30 °C, while the corresponding regular porphyrin **7** required above 100 °C for isomerization. Herein, we describe the unprecedented NH tautomerism-induced *cis-trans* isomerization of **1**. A plausible mechanism is discussed based on the kinetic and thermodynamic studies.

RESULTS AND DISCUSSION

Synthesis. The title compounds **1a** and **1b** were synthesized according to Scheme 2a. *p*-Trifluoromethylphenyl groups were employed as *meso*-substituents to make the NCP macrocycle more electron-deficient and acidic to form a stronger intramolecular hydrogen bond between the outer NH of the confused pyrrole and the pyridyl moiety in *cis*-form.[13] At first, N-confused tetrakis(*p*-trifluoromethylphenyl)porphyrin (**2**)[14] was treated with sodium cyanide in dimethylformamide (DMF) to yield 3-cyano-NCP (**3**). To avoid the aluminium metal insertion in the core during the reaction with diisobutylaluminium hydride (DIBAL-H), **3** was first metalated with nickel(II) acetate, and then reduced to 3-formyl-NCP Ni^{II} complex (**5**). Subsequent Wittig reaction afforded a mixture of *cis*- and *trans*-isomers of 3-[(2-pyridyl)ethenyl]-NCP Ni^{II} complexes (***cis*-1-Ni** and ***trans*-1-Ni**), both of which were isolated by silica gel column chromatography. Then, ***cis*-1-Ni** was demetalated with methanesulfonic acid to give a mixture of *cis*- and *trans*-isomers of freebase pyridylethenyl-NCPs (**1**), which were separated on a silica gel column. Notably, only ***cis*-2H-1** and ***trans*-3H-1** were isolated among the four possible isomers (Figure 1). Both ***cis*-1** and ***trans*-1** were recrystallized below 25 °C to avoid the isomerization. Furthermore, to fix to a 3H-model, ***trans*-3H-1a** was converted to the silver(III) complex, ***trans*-1a-Ag**, by treating with silver acetate (Scheme 2a).[7g] Likewise, the porphyrin derivative (**7**) was synthesized according to Scheme 2b.[15]

X-ray crystallography. Single crystal X-ray analyses of ***cis*-1a-Ni** and ***trans*-1a-Ag** were successfully performed (Figures 2 and S15, Table S6). As expected, ***cis*-1a-Ni** revealed the intramolecular hydrogen bond between the N atoms of the confused pyrrole ring and the pyridyl group, judging from the N····N atomic distance (2.718(7) Å), N····H-N angle (137.05°), and the dihedral angle between two rings (21.8°) (Figure 2a). Interestingly, the pyridyl ring of ***cis*-1a-Ni** shows the bond alternation with a value of harmonic-oscillator model for aromaticity (HOMA),[16] 0.520, which is remarkably smaller than that of the silver(III) complex, ***trans*-1a-Ag**, 0.901 (Figure 3). Thus, the aromaticity of the pyridyl ring seems largely affected by the hydrogen bonding between the pyridyl and confused pyrrole moieties in ***cis*-1a-Ni**. Furthermore, the bond length of the ethenyl double bond in ***cis*-1a-Ni** (1.351(7) Å) is longer than that of ***trans*-1a-Ag** (1.318(8) Å) (Figure 2b). This could be attributed to the extension of π-conjugation from the NCP macrocycle to the pyridyl moiety in ***cis*-1a-Ni** as schematically shown in Scheme 2 (bold blue line). This tendency was modestly reflected in the density functional theory (DFT) calculations on **1b**: the calculated bond lengths of ethenyl moieties were 1.363 and 1.351 Å for ***cis*-2H-1b** and ***trans*-3H-1b**, respectively (Figure S31). The effective π-conjugation through the 3-position of NCP has been illustrated with the divalent metal complexes of 2H-form.[17]

Scheme 2. Synthesis of a) Pyridylethenyl NCPs and b) Porphyrin (7)

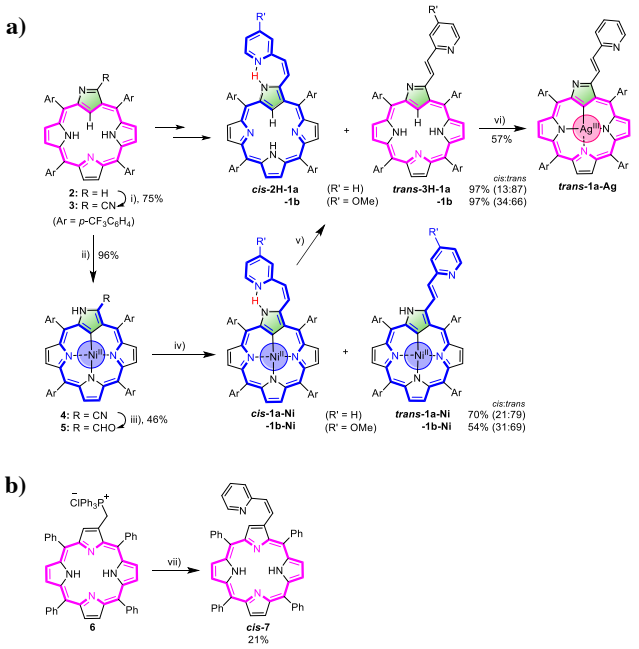

i) NaCN/DMF, ii) $Ni(acac)_2$/toluene/MeOH, iii) DIBAL-H/toluene, iv) $PyCH_2PPh_3Cl$, DBU/CH_2Cl_2, v) CH_3SO_3H/CH_2Cl_2, vi) AgOAc/CH_2Cl_2, vii) 2-formylpyridine, DBU/CH_2Cl_2.

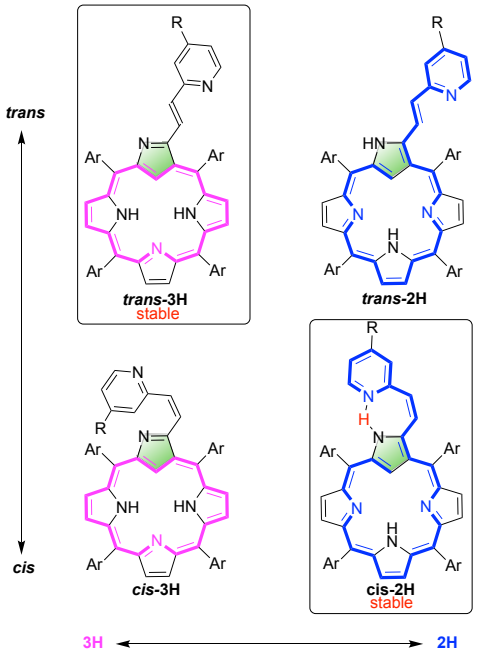

Figure 1. Possible isomers of **1**.

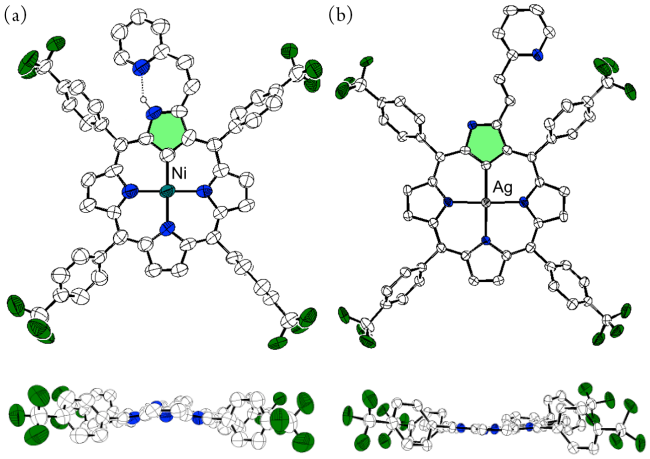

Figure 2. Top and side views of the X-ray structures of (a) ***cis*-1a-Ni** and (b) ***trans*-1a-Ag**, with 50% thermal ellipsoid probability. Hydrogen atoms except for the confused pyrrolic N–H are omitted for clarity.

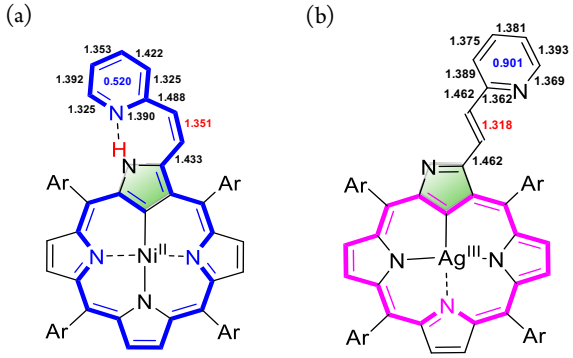

Figure 3. Selected bond lengths (Å) and HOMA values for pyridyl rings of (a) ***cis*-1a-Ni** and (b) ***trans*-1a-Ag**.

NMR study. *Cis* and *trans* isomers of **1** and **1-Ni** were identified by the coupling constants of the olefinic protons, $^3J_{cis}$ = 13.4–13.7 Hz and $^3J_{trans}$ = 15.5–16.5 Hz, respectively (Figure S16). The ^{1}H NMR spectra of **1-Ni** and the freebase **1** revealed the presence of strong intramolecular hydrogen bonding in the *cis*-isomers in $CDCl_3$. Namely, the signals of outer NH proton in ***cis*-1a-Ni** and ***cis*-1b-Ni** were observed at δ = 16.9 and 17.3 ppm, respectively, while the corresponding NH signals appeared at δ = 9.86 and 9.83 ppm in the case of ***trans*-1a-Ni** and ***trans*-1b-Ni**, respectively. The observed higher *cis*/*trans* ratio of **1b-Ni** (31:69) than **1a-Ni** (21:79) in the synthesis (Scheme 1) could be attributed to the stronger intramolecular hydrogen bonding in **1b-Ni**, pyridine moiety (R = OMe) of which is more basic. Similarly, the outer NH signals of the free bases, ***cis*-2H-1a** and ***cis*-2H-1b**, appeared at δ = 16.50 and 16.82 ppm, respectively (Figure S16a). The remaining ***trans*-3H** isomers, which lack the outer NH, showed the stronger aromaticity as indicated by the highly shielded inner CH signals at δ = –4.78 and –4.77 ppm for ***trans*-3H-1a** and ***trans*-3H-1b**, respectively (Figure S16b). The *cis*/*trans* ratio of the freebases **1a** and **1b** could not be determined accurately because of the facile isomerization during the work-up after demetalation of ***cis*-1-Ni**. Absence of other isomers, ***trans*-2H** and ***cis*-3H**, in the isolated products is probably due to their low stability resulting from a lack of intramolecular hydrogen bonding. Also, the repulsion between the lone pair electrons of two adjacent N atoms could not be ignored in the ***cis*-3H**.

Optical properties. The *cis*- and *trans*-isomers of **1** exhibited the distinct optical features. In the absorption spectra of the freebase **1** in CH_2Cl_2, the Soret-band of ***cis*-2H-1b** was observed at 495 nm, which was 23 nm red-shifted compared to ***trans*-3H-1b** (Figure 4). In addition, the spectral profiles in the Q-bands region of two isomers were largely different, reflecting the structural features of 2H- and 3H-tautomers.[5] This large shift is a characteristic of NCP derivatives, and was not seen with the regular porphyrin **7**, the shift of the Soret-band of which was only 5 nm (Figure S19). Interestingly, the emission of ***cis*-2H-1b** is significantly quenched compared with ***trans*-3H-1b** though both ***cis*-7** and ***trans*-7** showed intense fluorescence (Figures 4 and S19). The large differences in the optical properties between the isomers of **1** would be advantageous for the application such as molecular memory.

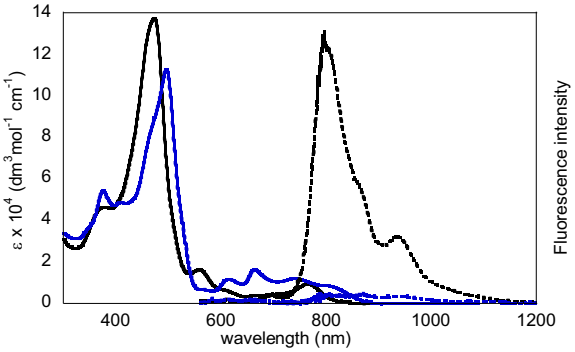

Figure 4. Absorption spectra of (a) ***trans*-3H-1b** (——) and (b) ***cis*-2H-1b** (——), and fluorescence spectra of (c) ***trans*-3H-1b** (-----) and (d) ***cis*-2H-1b** (-----) in CH_2Cl_2. Excited at 495 nm (*cis*) and 472 nm (*trans*).

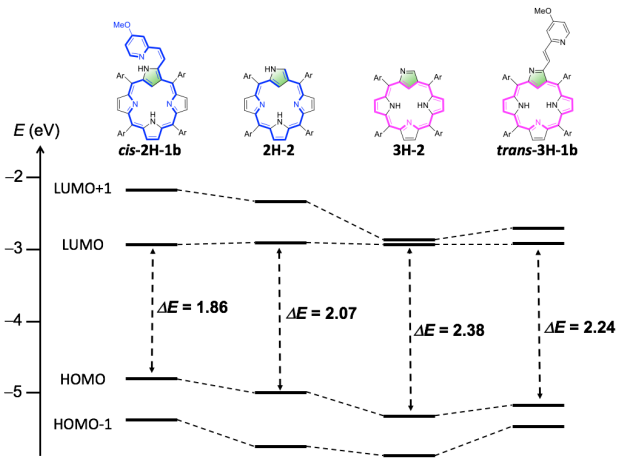

Figure 5. Molecular orbital energy diagrams of **1b** and **2** calculated at the B3LYP/6-31G** level.

Calculations. The nucleus independent chemical shift (NICS)[18] values of **1b** at the mass center of the macrocycle were calculated to be –5.09 ppm for ***cis*-2H** and –11.70 ppm for ***trans*-3H** (Figure S31). These results indicate that ***cis*-2H** is less aromatic than ***trans*-3H** in accordance with the previous report on NCPs.[5a] Molecular orbital energy diagrams of **1b** and reference NCP **2** are shown in Figure 5. ***Trans*-3H-1b** has comparatively degenerated LUMO and

LUMO+1, similar to **3H-2** or regular porphyrins. The 2H-type isomers have higher HOMO energies, and the pyridylethenyl substituent raises the HOMO and HOMO-1 levels of both ***cis*-2H-1b** and ***trans*-3H-1b**, and as a result, ***cis*-2H-1b** has a narrower HOMO-LUMO gap than ***trans*-3H-1b**. The time-dependent (TD)-DFT calculations showed the first excitation energy corresponding to the *Q*-band of **1b** is 832 nm for ***cis*-2H** and 694 nm for ***trans*-3H** (Figure S32-S33, Table S9). The difference in the Q-band transition between the *cis*/*trans* isomers of **1b** (138 nm) is much larger than that of **2** (60 nm), reflecting the conjugation pathway elongated to the pyridylethenyl-substituent in the ***cis*-2H-1b** (Table S10).

Thermal isomerization: Effects of concentration and added pyridine. The thermal *cis-trans* isomerization of **1** (Scheme 1c) was studied in CH_2Cl_2 using **1b** in the dark. Surprisingly, the isomerization proceeded very rapidly and occurred even at 30 °C, while the corresponding regular porphyrin ***cis*-7** required much higher temperature (≥100 °C in toluene-d_8) and ***trans*-Py-C=C-Pyr** did not show any sign of isomerization at 150 °C for 5 days (Figures 6, S27–28).

Notably, the isomerization of **1b** was significantly affected by its concentration as well as the pyridine added to the system (Figure 6). For [**1b**] = 15 μM, the initial rate (v_0) of isomerization from ***cis*-2H-1b** to ***trans*-3H-1b** was $v_0 = 7.42 \times 10^{-2}$ μM/min at 50 °C, whereas it decreased to 3.11×10^{-4} μM/min upon dilution ([**1b**] = 1.2 μM). Logarithmic plots of concentrations versus initial rates showed that the reaction order was ca. 2, indicating that two molecules of **1b** participated in the *cis-trans* isomerization (Figure 7a).

Apart from the above, when an excess amount of pyridine (25 mM) was added to the diluted solution ([**1b**] =1.2 μM), the isomerization reaction was accelerated by 10-fold ($v_0 = 3.10 \times 10^{-3}$ μM/min) (Figure 6). The logarithmic plots of pyridine concentrations versus initial rates showed a nonlinearly curved line, which suggests that there are at least two pathways of isomerization. The isomerization was not significantly affected by the low concentration of pyridine (reaction order of pyridine <0.1), while the isomerization was highly accelerated in the presence of a large amount of pyridine (>10 mM: reaction order of pyridine >1) (Figure 7b). In case of ***cis*-7**, the addition of pyridine did not function in the thermal isomerization under the similar conditions (at 50 °C in toluene-d_8). These results suggest that the pyridine molecule plays an important role in the transition state of this isomerization when an excess amount of pyridine is present in the solution.

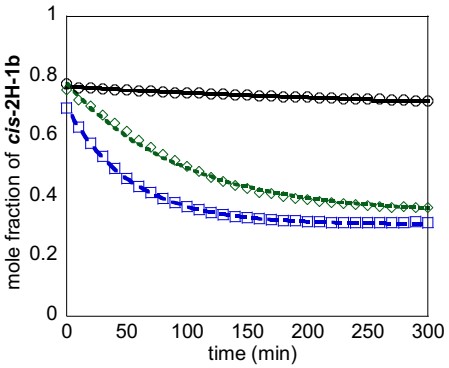

Figure 6. Time-courses of the thermal isomerization of **1b** in CH_2Cl_2 at 50 °C; [**1b**] = 1.2 μM (○), [**1b**] = 15 μM (□), and [**1b**] = 1.2 μM and [pyridine] = 25 mM (◇).

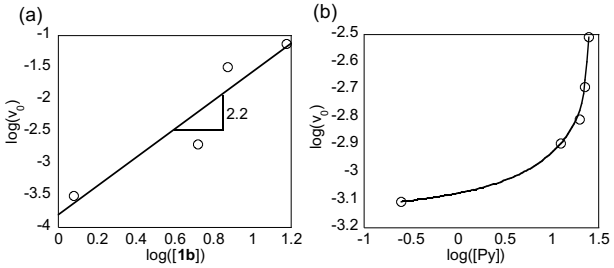

Figure 7. Logarithmic plots of (a) concentration of **1b** vs initial rate (v_0) and (b) pyridine concentration vs initial rate: [**1b**] =1.2 μM, measured by UV/Vis absorbance in CH_2Cl_2 at 50 °C.

Table 1. Isomerization Initial Rates of 1b (1.2 μM) with Various Additives (25 mM) in CH_2Cl_2 at 50 °C

Additive	Initial rate (v_0) (μM/min)	Relative initial rate (vs None)
None	3.11×10^{-4}	1
Pyridine	3.10×10^{-3}	9.97
2,6-Lutidine	2.58×10^{-4}	0.83
Quinoline	7.52×10^{-4}	2.42
Acridine	5.92×10^{-4}	1.90
4-Cyanopyridine	5.35×10^{-4}	1.72
4-Dimethylaminopyridine	5.36×10^{-4}	1.72

When 2,6-lutidine was added in place of pyridine, the acceleration was not observed or rather the isomerization was decelerated (Table 1, Figure S26). On the other hand, the addition of larger and planar pyridine derivatives, such as quinoline and acridine, accelerated the isomerization of **1b**, but the effects were significantly lower than pyridine. Furthermore, the addition of electron-rich (4-dimethylamino-) or electron-deficient (4-cyano-) pyridines also accelerated the isomerization but the effects were small in either case. These results may indicate the less steric hindrance and proper basicity are necessary for the additives to accelerate the isomerization, probably due to their two-way role, proton-capture and proton-transfer, in the NH tautomerism which coupled to the *cis-trans* isomerization. Moreover, for the thermal *cis-trans* isomerization of **1a-Ni**, which proceeded very slowly in toluene-d_8 at 100 °C and reached the equilibrium with the ratio of ***cis*-1a-Ni** : ***trans*-1a-Ni** = 79 : 21 after 60 days (Figure S20), the acceleration by the pyridine or its derivatives was not observed. In the pyridine titration experiments of ***trans*-1b-Ni** using ^{1}H NMR, the outer NH signal gradually shifted to a lower field region, while the other signals remained unchanged, indicating the hydrogen bonding between the outer NH and the added pyridine (Figure 8).

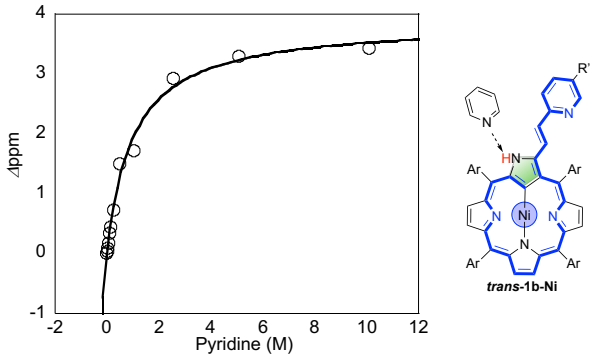

Figure 8. Changes of the chemical shifts of outer NH proton of ***trans*-1b-Ni** (5 mM) upon addition of pyridine-d_5 in $CDCl_3$. K = 0.99 M^{-1} was estimated from the curve fitting analysis.

Mechanism of the *cis-trans* isomerization. Characteristics of present isomerization system can be summarized as follows: 1) replacing a 6π pyrrole ring in **Py-C=C-Pyr** with a large 18π substituent, either NCP or porphyrin, is effective in decreasing the activation energy of the *cis-trans* isomerization, 2) free base NCP derivative isomerizes much faster than its nickel complex and corresponding porphyrin derivative, which implies the participation of NCP NH tautomerism in the isomerization process, 3) addition of pyridine to the system largely accelerates the isomerization, which suggests its dual role, proton capture and transfer, in the NH tautomerism of NCP moiety, 4) two **1b** molecules are involved in the isomerization, suggesting a similar role of the pyridyl moiety in **1b** as added pyridine.

To get the insight into the mechanism of present *cis-trans* isomerization, the thermodynamic energy profile of the system was first considered. Basically, three trails on the energy surface of the ground state were assumed for the isomerization of **1b** (Figure 9). One is path-**a**, in which proton transfer (PT) and olefin rotation (OR) proceed concertedly. Others are path-(**b**→**c**) and path-(**d**→**e**), in which PT-OR or OR-PT proceeds stepwise (Figure 9A). Namely, the path-**b** and path-**e** correspond to the NH tautomerism (PT) and the path-**c** and path-**d** are *cis-trans* isomerization (OR) process. Calculations on the transition states of each path were so far difficult, thus, we simply compared the relative energies of the hypothetical structures in the transition state where the olefin moiety is twisted by 90° (Figure 10, Table S7). For path-**c** and path-**d**, $\Delta G_o^{\ddagger}{}_{\text{path-c}}$ = 37.5 kcal/mol and $\Delta G_o^{\ddagger}{}_{\text{path-d}}$ = 40.1 kcal/mol (vs ΔG_o *trans*-**3H** = 0 kcal/mol) were obtained. On the other hand, for path-**b** and path-**e**, we adapted the values of $\Delta G_o^{\ddagger}{}_{3H\rightarrow 2H}$ = 29.9 kcal/mol and $\Delta G_o^{\ddagger}{}_{2H\rightarrow 3H}$ = 28.5 kcal/mol, which were derived from the NH tautomerism of N-confused tetraphenylporphyrin (NCTPP) (*vide infra*).[19] By using these values, we can schematically depict the energy profiles of isomerization for each pathway as shown in Figure 9B. In the stepwise cases, the activation energies of OR processes are larger than those of NH tautomerism, indicating that OR (path-**c** and path-**d**) is the rate-determining step. However, the results that the addition of pyridine accelerated the *cis-trans* isomerization of **1b** but not **1a-Ni** would not be compatible with the stepwise mechanism if the rate-determining steps are the same OR process in the both systems.

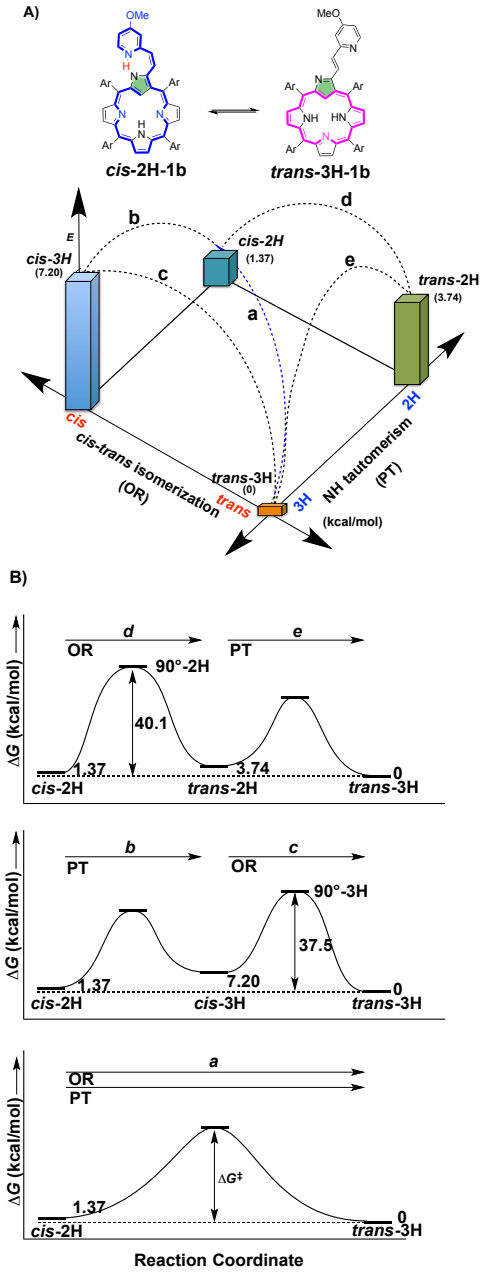

Figure 9. Schematic illustration of free energy profiles of *cis-trans* isomerization and NH tautomerism between ***cis*-2H-1b** and ***trans*-3H-1b**. **OR**: olefin rotation, **PT**: proton transfer.

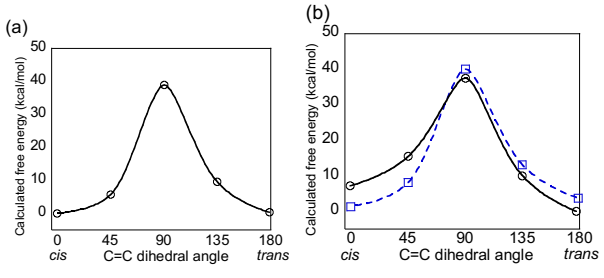

Figure 10. Calculated Gibbs free energies of (a) **1a-Ni** (–⊙–) and (b) 2H form of **1b**: (--⊡--) and 3H form of **1b**: (–⊙–) with various dihedral angles of olefin moiety (B3LYP/6-31G** for C, H, F, N, and LanL2DZ for Ni).

In order to estimate the activation parameters of independent pathways of NH tautomerism (path-**b** and path-**e**), we measured the rate constants of NCTPP tautomerism in the pyridine-d_5/$CDCl_3$ mixture solutions. This mixed solvent system was selected for the concurrent detection of 2H- and 3H-tautomers by ^{1}H NMR, since the 3H-type tautomer is predominantly formed in the CD_2Cl_2 or $CDCl_3$ only solution due to the higher stability of the 3H-type than 2H-tautomer.[5a] The values of $\Delta G_o^{\ddagger}{}_{3H\rightarrow 2H}$ = 29.9 kcal/mol and $\Delta G_o^{\ddagger}{}_{2H\rightarrow 3H}$ = 28.0 kcal/mol at 298 K in $CDCl_3$ only solution were derived from the plots of $\Delta G_o^{\ddagger}$ against the pyridine concentrations, by extrapolating to the point at [pyridine-d_5] = 0 (Figure 11, Table 2). These values are much higher than the NH tautomerism of regular porphyrin ($\Delta G_o^{\ddagger}$ ~12 kcal/mol) where the tautomerism occurs only inside of the core.[20] The larger $\Delta G_o^{\ddagger}$ of NCP should be explained by the different mechanism from the tunneling model of the regular porphyrin.[21] Because of the solvent dependence of $\Delta G_o^{\ddagger}$ and the long-range proton transfer from the inner to the outer, a possibility of ring rotation mechanism was proposed based on the calculation study[22] but the detailed mechanism of NH tautomerism of NCP still remains challenging.

From the variable-temperature kinetic experiments, the activation free energy of the thermal isomerization of **1b** from *cis* to *trans* was determined to be $\Delta G_o^{\ddagger}{}_{cis\rightarrow trans}$ = 35.7 kcal/mol, while that of **1a-Ni** was 42.3 kcal/mol at high concentration ([**1b**]: 680 μM, [**1a-Ni**]: 1.8 mM) (Tables S1, S3). The calculated free energy differences for the hypothetical OR transition states of **1b** and **1a-Ni** are similar values of 38.7 and 38.9 kcal/mol, respectively (Figure 9, Table S7).[23] The compound **7** showed the similar trend with the energy differences of 35.4~39.0 kcal/mol (Figure S30 and Table S8). Thus, the large decrease of activation energy of **1b** from that of Ni complex ($\Delta\Delta G_o^{\ddagger}{}_{cis\rightarrow trans}$ = 6.6 kcal/mol) could be attributed to the NH tautomerism during the *cis-trans* isomerization. Here, it should be noted that the added pyridine accelerates the NH tautomerism of NCP, that is, lowers the activation energy of NH tautomerism, probably by mediating the proton migration (Table 2). If the pyridine participated in both the tautomerism and *cis-trans* isomerization to assist the breaking of the intramolecular hydrogen bonding in ***cis*-2H-1b** and twisting the pyridylethenyl moiety favorable for the *cis-trans* isomerization through the steric repulsion (Scheme 3), then, the rotation of C=C double bond and proton transfer occur concertedly, which could reduce the activation energy of double bond rotation lower than the stepwise pathways. Although the above mechanism is highly speculative and needs more detailed studies including calculations, it is likely that PT process is merged with the OR process (path-**a**) to account for the acceleration of the *cis-trans* isomerization reaction. Considering the observed result that the isomerization is second-order to the concentration of **1b**, it is highly probable that the pyridine moiety in ***trans*-3H-1b** plays the similar role as added pyridine in the *cis-trans* isomerization.

Table 2. Activation Parameters of NH Tautomerism of NCTPP (3H → 2H)

solvents	$\Delta G_o^{\ddagger}{}_{3H\rightarrow 2H}$ [kcal/mol]	$\Delta H_o^{\ddagger}{}_{3H\rightarrow 2H}$ [kcal/mol]	$\Delta S_o^{\ddagger}{}_{3H\rightarrow 2H}$ [cal/mol·K]
Pyridine-d_5	16.12	1.93	−47.6
50% Pyridine-d_5 / $CDCl_3$	24.58	16.40	−27.5
30% Pyridine-d_5 / $CDCl_3$	25.31	21.19	−13.8
$CDCl_3$	30.32*	29.83*	−1.59*

*Obtained from extrapolation of the plot lines in Figure 11.

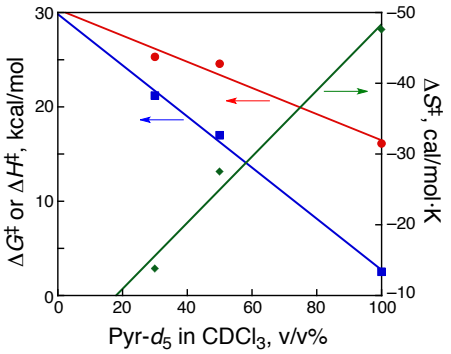

Figure 11. The activation parameters of the NH tautomerism of NCTPP (20 mM) in pyridine-d_5 (Pyr-d_5)/$CDCl_3$. $\Delta G_o^{\ddagger}$ (●), $\Delta H_o^{\ddagger}$ (■), $\Delta S_o^{\ddagger}$ (◆).

Scheme 3. A Plausible Isomerization Mechanism of 1 in the Presence of Pyridine

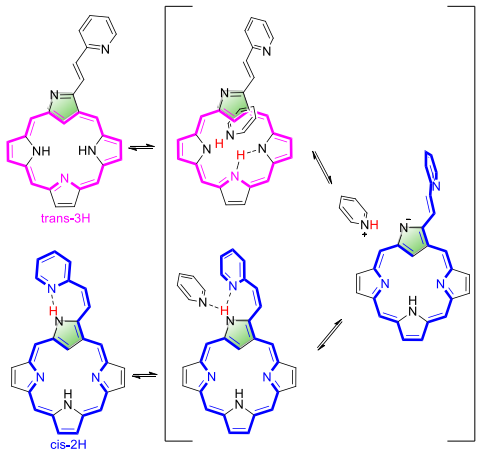

Photo-isomerization. Lastly, photoisomerization of **1b** was investigated by monitoring the fluorescence changes at 20 °C, where the thermal isomerization was negligible (Figure 12). Upon irradiation at the Soret band (496 nm) of ***cis*-2H-1b**, isomerization to ***trans*-3H-1b** proceeded with the initial rate of $v_0 = 8.12 \times 10^{-4}$ μM/min. At the photostationary state, the ratio of isomers, ***cis*-2H** : ***trans*-3H**, reached ca. 6 : 4, which is different from that of thermal isomerization, 4 : 6, at 30 °C. The acceleration effect of added pyridine in this photoisomerization system was modest compared with the thermal

one. In the case of **Py-C=C-Pyr**, the excited state intramolecular proton transfer (ESIPT) mechanism[24] was demonstrated in the photoisomerization.[3] Thus, in the present isomerization, there is a possibility of ESIPT from the confused pyrrole to the pyridyl moiety of ***cis*-2H-1b** under photo-irradiation. For a further discussion, however, the fast time-resolved spectroscopic study is indispensable.

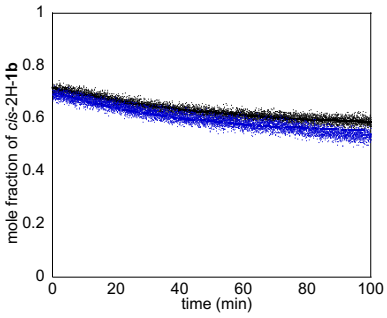

Figure 12. Time-courses of the photoisomerization of **1b** (1.2 μM) monitored by the fluorescence at 800 nm in CH_2Cl_2 at 20 °C upon irradiation at 496 nm: (a) without pyridine (black) and (b) with excess pyridine (25 mM) (blue).

CONCLUSION

In summary, we have synthesized a novel type of diarylethenes, *cis*- and *trans*-pyridylethenyl N-confused porphyrins (**1**) and investigated the thermal *cis-trans* isomerization in detail. The *cis*-isomer was largely stabilized by the intramolecular hydrogen bonding between the pyrrolic-NH of NCP and the pyridinic-N in the vicinity. The freebase **1** isomerized readily even at 30 °C, accompanied by the NH tautomerism of NCP moiety. The isomerization was accelerated by increasing the concentration of **1** or by the addition of pyridine. The kinetic studies revealed the isomerization reaction was second order and the activation energy of this thermal isomerization from *cis*- to *trans*-isomer was $\Delta G^{\ddagger}_{o\,cis\rightarrow trans}$ = 35.7 kcal/mol at 298 K, which is much smaller than that of Ni complex, 42.3 kcal/mol. In addition, photoisomerization was also observed at 20 °C, where the thermal isomerization was negligible. The coupling of NCP tautomerism and *cis-trans* isomerization enabled us to develop a new isomerization system that affords two interchangeable isomers, electronic properties of which are significantly different. The present study demonstrated the design of diarylethene, *to make the two aryl groups bifunctional and interactive each other in the cis-form*, is effective to cause the change of tautomer's electronic state largely, and the NCP could serve as an *expanded pyrrole* and/or *expanded pyridine*.

EXPERIMENTAL SECTION

General Methods. Commercially available solvents and reagents were used without further purification unless otherwise mentioned. Thin-layer chromatography (TLC) was carried out on aluminum sheets coated with silica gel 60 F254 (MERCK). Preparative separation was performed by silica gel flash column chromatography (KANTO Silica Gel 60 N, spherical, neutral, 40–50 μm) or silica gel gravity column chromatography (KANTO Silica Gel 60 N, spherical, neutral, 63–210 μm). ^{1}H NMR spectra were recorded on a JNM-AL 300 FT-NMR spectrometer (JEOL) at 300 MHz, and chemical shifts were reported relative to a residual proton of a deuterated solvent, $CHCl_3$ (δ = 7.26) in ppm. ^{13}C NMR spectra were recorded at either 75 MHz (JNM-AL 300) or 150 MHz (Bruker AVANCE III 600) and chemical shifts were reported relative to either $CDCl_3$ (δ = 77.13) or THF-d_8 (δ = 25.31) in ppm. ^{19}F NMR spectra were recorded on a JNM-AL 300 (270 MHz) and chemical shifts were reported relative to perfluorobenzene (δ = –164.9) in ppm. UV/vis absorption spectra were recorded on a UV-3150PC spectrometer (Shimadzu). Fluorescence spectra were recorded on an SPEX Fluorolog spectrometer (HORIBA) with photomultiplier module (Hamamatsu R928P) and InGaAs photodiode array. High-resolution mass spectra were measured with a JMS-T100CS (ESI-TOF mode, JEOL). Absolute quantum yields of emission were measured with PL quantum yield measurement system (C9920-02, Hamamatsu).

Time-course measurements of isomerization. Time-course studies of the thermal *cis-trans* isomerization were performed by following the changes in the ^{1}H NMR spectra (at high concentration) or UV/vis absorption spectra (at low concentration). Integration of olefinic proton signals or intensity of the Soret-band was used to calculate the *cis*/*trans* molar ratios. Sample solution was prepared by dissolving the pure isomer in the cold solvent to suppress the isomerization before measurements. The sealed NMR tube or tightly capped UV cell was placed into the thermostat bath. The first point was measured immediately after reaching the desired temperature. Because of the facile isomerization of the free base **1b**, the compound has already isomerized at the first measurement point (ca. 0.2 molar ratio).

Synthesis. N-confused tetrakis(*p*-trifluoromethylphenyl)-porphyrin (**2**): To a 3 L flask, CH_2Cl_2 (3 L), pyrrole (2 mL), and 4-(trifluoromethyl)benzaldehyde (4 mL) were added. The reaction was initiated by addition of methanesulfonic acid (1.4 mL). The reaction mixture was stirred at room temperature for 30 min. DDQ (6.0 g) was added and the mixture was allowed to stir for 2 min and then the acid was quenched by addition of triethylamine (12 mL). Impurity was removed by passage through alumina and silica gel. After evaporation, the residue was separated by silica gel column chromatography with 10% hexane in CH_2Cl_2. Concentration of the fraction and recrystallization of the residue from CH_2Cl_2/hexane afforded **2**. Yield: 1.57 g (24%). ^{1}H NMR ($CDCl_3$, 300 MHz, ppm): δ –5.11 (s, 1H, inner CH), –2.50 (br s, 2H, inner NH), 8.05 (d, J = 7.5 Hz, 4H, *m*-ArH), 8.12 (d, J = 8.3 Hz, 2H, *m*-ArH), 8.14 (d, J = 8.9 Hz, 2H, *m*-ArH), 8.28 (d, J = 7.5 Hz, 2H, *o*-ArH), 8.30 (d, J = 7.5 Hz, 2H, *o*-ArH), 8.45 (d, J = 8.9 Hz, 2H, *o*-ArH), 8.48 (d, J = 8.3 Hz, 2H, *o*-ArH), 8.52 (d, J = 5.1 Hz, 1H, β-H), 8.55 (d, J = 5.1 Hz, 1H, β-H), 8.57 (d, J = 5.0 Hz, 1H, β-H), 8.62 (d, J = 5.0 Hz, 1H, β-H), 8.75 (s, 1H, α-H), 8.93 (d, J = 5.0 Hz, 1H, β-H), 8.98 (d, J = 5.0 Hz, 1H, β-H); ^{13}C NMR ($CDCl_3$, 75 MHz, ppm): δ 99.0, 116.3, 117.9, 122.30, 122.32, 122.4, 123.3, 123.77, 123.81, 123.83, 123.85, 123.88, 123.93, 124.07, 124.10, 124.14, 124.2, 124.34, 124.36, 124.38, 124.41, 124.44, 124.48, 125.41, 125.44, 125.46, 125.51, 125.54, 125.55, 125.59, 125.90, 125.93, 126.1, 126.36, 126.40, 126.44, 126.5, 127.8, 127.90, 127.93, 127.95, 127.99, 128.23, 128.25, 128.27, 128.31, 128.34, 129.51, 129.53, 129.77, 129.87, 129.92, 130.1, 130.2, 130.3, 130.4, 130.6, 133.7, 134.29, 134.36, 134.41, 134.5, 135.0, 136.4, 136.51, 136.59, 136.66, 136.70, 136.9, 139.0, 139.7, 142.28, 142.30, 142.45, 142.47, 144.72, 144.73, 144.76, 144.77, 149.1, 155.8, 156.8; Due to the severe spectral complexity in the sp^2-carbon region, the ^{13}C-F coupled splitting

could not be assigned. ^{19}F NMR ($CDCl_3$, 270 MHz): δ –60.48 (s, 3F, CF_3), –60.52 (s, 6F, CF_3), –60.57 (s, 3F, CF_3); UV-vis (CH_2Cl_2, λ_{max}/nm (ε)): 724 (10500), 581 (11600), 540 (10400), 440(176000); HRMS (ESI-TOF) *m/z*: $[M+H]^+$ Calcd for $C_{48}H_{26}F_{12}N_4$ 887.20441; Found 887.20283.

3-Cyano-N-Confused Tetrakis(*p*-trifluoromethylphenyl)-porphyrin (3): To a 500 mL DMF solution of **2** (400 mg, 0.45 mmol), sodium cyanide (322 mg, 10 mmol) was added and stirred for 12 h. After the solvent was evaporated, the residue was dissolved in CH_2Cl_2 and the solution was washed with water and brine. The organic layer was separated and dried over Na_2SO_4. After evaporation, the residue was separated by silica gel column chromatography with CH_2Cl_2/hexane. Concentration of the fraction and recrystallization of the residue from CH_2Cl_2/MeOH afforded **3**. Yield: 308 mg (75%). ^{1}H NMR ($CDCl_3$, 300 MHz, ppm): δ –4.42 (s, 1H, inner CH), –1.60 (br s, 2H, inner NH), 8.04 (d, *J* = 7.9 Hz, 2H, *m*-ArH), 8.05 (d, *J* = 7.9 Hz, 2H, *m*-ArH), 8.12 (d, *J* = 8.2 Hz, 2H, *m*-ArH), 8.14 (d, *J* = 8.5 Hz, 2H, *m*-ArH), 8.23 (d, *J* = 7.9 Hz, 2H, *o*-ArH), 8.26 (d, *J* = 7.9 Hz, 2H, *o*-ArH), 8.38–8.43 (m, 4H, *o*-ArH, *β*-H), 8.44 (d, *J* = 7.9 Hz, 2H, *o*-ArH), 8.47 (d, *J* = 5.1 Hz, 1H, *β*-H), 8.51 (d, *J* = 5.2 Hz, 1H, *β*-H), 8.90 (d, *J* = 5.2 Hz, 1H, *β*-H), 8.92 (d, *J* = 5.1 Hz, 1H, *β*-H); ^{13}C NMR ($CDCl_3$, 75 MHz, ppm): δ 93.6, 115.2, 116.3, 118.1, 118.6, 122.18, 122.23, 122.3, 123.87, 123.97, 124.00, 124.05, 124.10, 124.12, 124.17, 124.20, 124.21, 124.24, 124.26, 124.31, 124.36, 124.38, 124.64, 124.67, 124.70, 124.74, 124.78, 124.80, 124.83, 124.85, 124.86, 124.89, 124.91, 125.79, 125.83, 125.9, 126.02, 126.07, 126.11, 126.13, 126.16, 127.28, 127.29, 127.31, 127.35, 127.41, 129.40, 129.44, 129.49, 129.69, 129.71, 129.77, 129.83, 129.89, 139.95, 130.1, 130.2, 130.3, 130.4, 130.57, 130.63, 130.8, 130.96, 130.99, 131.2, 131.3, 131.4, 131.8, 134.3, 134.4, 135.16, 135.19, 135.25, 135.29, 135.33, 135.79, 135.83, 135.9, 136.1, 137.0, 137.3, 137.5, 141.3, 141.4, 141.50, 141.52, 141.8, 142.6, 144.00, 144.02, 146.3, 157.6, 159.0; ^{19}F NMR ($CDCl_3$, 270 MHz): δ –60.53 (s, 3F, CF_3), –60.61 (s, 6F, CF_3), –60.63 (s, 3F, CF_3); UV-vis (CH_2Cl_2, λ_{max}/nm (ε)): 774 (16500), 596 (3250), 551 (13500), 455 (186000), 387 (44700); Anal. Calcd for 2c ($C_{49}H_{25}F_{12}N_5$): C 64.55; H 2.76; N 7.68. Found: C 64.63; H 2.82; N 7.47.

3-Cyano-N-Confused Tetrakis(*p*-trifluoromethylphenyl)-porphyrin Ni(II) Complex (4): Compound **3** (300 mg, 0.33 mmol) and nickel acetylacetate (452 mg) were dissolved in toluene/ methanol and refluxed for 4 h under Ar atmosphere. The reaction mixture was washed with water and the separated organic layer was dried over Na_2SO_4. (Quick work up was necessary to avoid the decomposition of the product.) The solvent was evaporated and the residue was recrystallized from CH_2Cl_2/hexane to afford **4**. Yield: 297 mg (96%). ^{1}H NMR ($CDCl_3$, 300 MHz, ppm): δ 7.21 (d, *J* = 5.5 Hz, 1H, *β*-H), 7.29 (d, *J* = 5.2 Hz, 1H, *β*-H), 7.43 (d, *J* = 5.2 Hz, 1H, *β*-H), 7.45 (d, *J* = 5.2 Hz, 1H, *β*-H), 7.49 (d, *J* = 5.5 Hz, 1H, *β*-H), 7.53 (d, *J* = 4.9 Hz, 1H, *β*-H), 7.75–7.87 (m, 14H, *o*,*m*-ArH), 7.93 (d, *J* = 7.9 Hz, 2H, *o*-ArH); ^{13}C NMR (THF-d_8, 75 MHz, ppm): δ 115.9, 116.7, 117.5, 122.40, 122.43, 122.46, 123.75, 123.77, 123.81, 123.86, 123.90, 123.95, 124.00, 124.02, 124.05, 124.09, 124.13, 124.18, 124.19, 124.6, 126.00, 126.03, 126.06, 128.6, 129.01, 129.08, 129.12, 129.17, 129.4, 129.57, 129.60, 129.63, 129.66, 129.69, 129.72, 129.74, 129.76, 129.80, 129.81, 129.86, 129.91, 130.0, 130.1, 130.6, 131.6, 132.4, 132.60, 132.63, 132.71, 132.76, 132.78, 133.15, 133.24, 133.69, 134.31, 134.33, 134.35, 134.37, 134.39, 134.41, 134.45, 140.6, 141.8, 144.03, 144.05, 144.1, 146.6, 146.9, 150.5, 151.5, 155.0, 156.3, 190.7; ^{19}F NMR ($CDCl_3$, 270 MHz): δ –65.46 (s, 6F, CF_3), –65.48 (s, 3F, CF_3), –65.67 (s, 3F, CF_3); UV-vis (CH_2Cl_2, λ_{max}/nm (ε)): 913 (2050), 815 (2620), 651 (7180), 569 (8630), 527 (5720), 429 (55000), 356 (41400); Anal. Calcd for **3c** ($C_{49}H_{23}F_{12}N_5Ni$): C 60.77; H 2.39; N 7.23. Found: C 60.38; H 2.34; N 7.15.

3-Formyl-N-Confused Tetrakis(*p*-trifluoromethylphenyl)-porphyrin Ni(II) Complex (5): To a 260 mL solution of **4** (370 mg, 0.38 mmol) in toluene, 1.0 M DIBAL-H in toluene (2.3 mL, 2.3 mmol) was added under nitrogen at 0 °C. After 5 min, the reaction was quenched by 5 mL of 1.0 M hydrochloric acid and the solution was stirred at 0 °C for 30 min. The organic layer was washed with water and dried over Na_2SO_4. After evaporation, the residues were separated by silica gel column chromatography with CH_2Cl_2/hexane. The fraction was concentrated and the residue was recrystallized from MeOH/CH_2Cl_2 to give **5**. Yield: 170 mg (46%). ^{1}H NMR ($CDCl_3$): δ 7.13 (d, *J* = 4.9 Hz, 1H, *β*-H), 7.19 (d, *J* = 5.2 Hz, 1H, *β*-H), 7.36 (s, 2H, *β*-H), 7.41 (d, *J* = 4.9 Hz, 1H, *β*-H), 7.42 (d, *J* = 5.2 Hz, 1H, *β*-H), 7.70 (d, *J* = 8.4 Hz, 2H, *m*-ArH), 7.72 (d, *J* = 8.4 Hz, 2H, *m*-ArH), 7.76 (d, *J* = 8.4 Hz, 2H, *m*-ArH), 7.78 (d, *J* = 8.4 Hz, 4H, *o*,*m*-ArH), 7.85 (d, *J* = 8.4 Hz, 2H, *o*-ArH), 8.46 (s, 1H, CHO), 9.97 (br s, 1H, outer NH); ^{13}C NMR ($CDCl_3$, 75 MHz, ppm): δ 117.0, 117.3, 120.3, 120.8, 122.15, 122.20, 122.5, 123.96, 124.01, 124.07, 124.25, 124.28, 124.33, 124.37, 124.42, 124.68, 124.75, 124.79, 124.84, 125.01, 125.02, 125.3, 125.4, 125.76, 125.81, 126.1, 129.3, 129.7, 130.0, 130.5, 130.9, 131.0, 131.1, 131.4, 131.6, 132.42, 132.48, 132.54, 132.8, 133.31, 133.34, 133.4, 133.6, 134.0, 134.6, 134.7, 139.5, 139.6, 143.0, 143.29, 143.32, 143.39, 143.41, 143.8, 148.6, 148.7, 152.2, 152.9, 157.5, 158.6, 180.7; ^{19}F NMR ($CDCl_3$, 270 MHz): δ –60.71 (s, 6F, CF_3), –60.74 (s, 3F, CF_3), –60.92 (s, 3F, CF_3); UV-vis (CH_2Cl_2, λ_{max}/nm (ε)): 867 (872), 672 (5310), 587 (12600), 545 (6730), 437 (54300), 366 (46700); HRMS (ESI-TOF) *m/z*: $[M-H]^-$ Calcd for $C_{49}H_{24}F_{12}N_4NiO$ 969.10296; Found 969.10337.

((4-Methoxypyridin-2-yl)methyl)-triphenylphosphonium Chloride: 2-Hydroxymethyl-4-methoxypyridine[23] (100 mg, 0.72 mmol) was dissolved in CH_2Cl_2 (3 mL) and treated with thionyl chloride (0.063 mL) at room temperature for 1 h. The reaction mixture was neutralized with saturated aqueous $NaHCO_3$ solution, extracted with CH_2Cl_2, and dried over Na_2SO_4. After evaporation, 2-chloromethyl-4-methoxypyridine was obtained. This was reacted with an equimolar amount of triphenylphosphine in toluene (2 mL) at reflux for 21 h. The solvent was evaporated and the residue was washed with ether to give a 170 mg of Wittig reagent after drying *in vacuo*. ^{1}H NMR ($CDCl_3$): δ 3.78 (s, 3H, CH_3), 5.65 (d, *J* = 14 Hz, 2H, CH_2), 6.60 (d, *J* = 6.0 Hz, 1H, Py), 7.58–7.89 (m, 16H, Ph and Py), 8.0 (d, *J* = 6.0 Hz, 1H, Py); ^{13}C NMR ($CDCl_3$, 75 MHz): δ 32.6 (d, $J_{C\text{-}P}$ = 51.7 Hz, CH_2-P), 55.9 (s, CH_3), 111.0 (s, C(H), Py), 111.9 (d, $J_{C(3)\text{-}P}$ = 8.1 Hz, C(3), Py), 119.0 (d, $J_{c(i)\text{-}P}$ = 86.55 Hz, C(*i*), Ph), 129.8 (d, $J_{C(o)\text{-}P}$ = 12.5 Hz, C(*o*), Ph), 134.3 (d, $J_{C(m)\text{-}P}$ = 10.0 Hz, C(*m*), Ph), 134.5 (d, $J_{C(p)\text{-}P}$ = 3.1 Hz, C(*p*), Ph), 149.2 (s, C(H), Py), 151.8 (d, $J_{C(2)\text{-}P}$ = 8.1 Hz, C(2), Py), 166.3 (s, C(H), Py).

3-(2-(2-Pyridyl)ethenyl)-N-Confused Tetrakis(*p*-trifluoromethylphenyl)porphyrin Ni(II) Complex (1a-Ni): Compound **5** (20 mg, 0.021 mmol) and triphenyl(pyridin-2-ylmethyl)phosphonium chloride (8 mg, 0.021 mmol) were dissolved in CH_2Cl_2 (15 mL) and DBU (3.1 μL, 0.021 mmol) was added. The solution was stirred for 15 min at room temperature.

The resulting solution was evaporated and the residue was separated by silica gel column chromatography with CH_2Cl_2/hexane. The first and third fractions were recrystallized from CH_2Cl_2/hexane to give ***cis*-1a-Ni** and ***trans*-1a-Ni**, respectively. Yield: ***cis*-1a-Ni,** 3.3 mg (15%), ***trans*-1a-Ni,** 12.0 mg (55%). ***cis*-1a-Ni**: ^{1}H NMR ($CDCl_3$): δ 6.17 (d, J = 13.7 Hz, 1H, olefin), 6.30 (d, J = 13.7 Hz, 1H, olefin), 6.96 (dd, J = 5.2, 1.5 Hz, 1H, Py), 7.09 (dd, J = 7.0, 5.2 Hz, 1H, Py), 7.34 (d, J = 8.5 Hz, 1H, Py), 7.61 (d, J = 5.2 Hz, 1H, β-H), 7.66 (d, J = 5.5 Hz, 1H, β-H), 7.74 (ddd, J = 7.5, 7.5, 2.7 Hz, 1H, Py), 7.77 (d, J = 5.5 Hz, 1H, β-H), 7.78 (d, J = 5.2 Hz, 1H, β-H), 7.78 (d, J = 5.5 Hz, 2H, β-H), 7.85 (d, J = 7.5 Hz, 2H, m-ArH), 7.94 (d, J = 7.5 Hz, 2H, o-ArH), 7.84 (d, J = 6.9 Hz, 2H, m-ArH), 7.87 (d, J = 7.5 Hz, 2H, m-ArH), 7.92 (d, J = 6.9 Hz, 2H, o-ArH), 7.96 (d, J = 7.5 Hz, 2H, o-ArH), 7.98 (d, J = 7.9 Hz, 2H, m-ArH), 8.16 (d, J = 7.9 Hz, 2H, o-ArH), 16.9 (br s, 1H, outer NH); ^{13}C NMR ($CDCl_3$, 150 MHz): δ 116.1, 117.1, 121.3, 121.6, 122.8, 123.1, 123.39, 123.46, 123.52, 124.00, 124.02, 124.10, 124.13, 124.16, 124.19, 124.21, 124.47, 124.49, 124.52, 125.19, 125.27, 125.33, 127.58, 127.61, 129.1, 129.3, 129.6, 129.8, 130.17, 130.23, 130.39, 130.44, 130.7, 131.4, 132.3, 132.4, 133.22, 133.24, 133.3, 133.7, 133.8, 138.1, 143.3, 144.7, 144.8, 145.0, 145.5, 146.3, 146.8, 148.1, 149.2, 151.5, 152.7, 152.8, 152.8; ^{19}F NMR ($CDCl_3$, 270 MHz): δ –60.46 (s, 3F, CF_3), –60.50 (s, 3F, CF_3), –60.51 (s, 3F, CF_3), –60.75 (s, 3F, CF_3); UV-vis (CH_2Cl_2, λ_{max} (nm)) 800 (3900), 616 (21900), 492 (37000), 454 (40200), 393 (38600); HRMS (ESI-TOF) m/z: $[M]^+$ Calcd for $C_{55}H_{29}F_{12}N_5Ni$ 1045.15848; Found 1045.15846. ***trans*-1a-Ni**: ^{1}H NMR ($CDCl_3$): δ 6.72 (d, J = 16.5 Hz, 1H, olefin), 6.95 (d, J = 8.2 Hz, 1H, Py), 7.08 (d, J = 16.5 Hz, 1H, olefin), 7.19 (dd, J = 7.0, 4.9 Hz, 1H, Py), 7.60 (d, J = 5.4 Hz, 1H, β-H), 7.62 (ddd, J = 7.8, 7.8, 1.5 Hz, 1H, Py), 7.67 (d, J = 5.2 Hz, 1H, β-H), 7.76 (d, J = 5.1 Hz, 1H, β-H), 7.80 (d, J = 5.1 Hz, 1H, β-H), 7.81 (d, J = 5.4 Hz, 1H, β-H), 7.83 (d, J = 5.2 Hz, 1H, β-H), 7.85 (d, J = 9.0 Hz, 2H, m-ArH), 7.86 (d, J = 9.0 Hz, 2H, m-ArH), 7.91 (d, J = 9.0 Hz, 2H, m-ArH), 7.94 (d, J = 9.0 Hz, 4H, o-ArH), 7.99 (d, J = 9.0 Hz, 2H, o-ArH), 7.97 (d, J = 9.0 Hz, 2H, m-ArH), 8.03 (d, J = 9.0 Hz, 2H, o-ArH), 8.53 (d, J = 4.0 Hz, 1H, Py), 9.86 (br s, 1H, outer NH); ^{13}C NMR ($CDCl_3$, 75 MHz): δ 116.3, 117.6, 119.9, 121.28, 121.32, 121.8, 122.4, 122.6, 122.7, 123.6, 124.30, 124.35, 124.38, 124.43, 134.5, 125.05, 125.10, 125.14, 125.2, 126.0, 126.2, 126.3, 126.5, 129.5, 129.6, 129.8, 130.1, 130.2, 130.4, 130.6, 130.8, 130.9, 131.3, 131.8, 132.3, 132.5, 132.7, 132.9, 133.3, 133.6, 134.0, 136.7, 141.1, 144.6, 144.71, 144.73, 145.2, 146.6, 148.6, 150.01, 150.08, 152.1, 152.6, 153.9, 154.0; ^{19}F NMR ($CDCl_3$, 270 MHz): δ –60.53 (s, 3F, CF_3), –60.54 (s, 3F, CF_3), –60.52 (s, 3F, CF_3), –60.68 (s, 3F, CF_3); UV-vis (CH_2Cl_2, λ_{max}/nm (ε)): 800 (4190), 602 (30200), 452 (68500), 382 (61200); HRMS (ESI-TOF) m/z: $[M-H]^-$ Calcd for $C_{55}H_{29}F_{12}N_5Ni$ 1044.15083; Found 1044.15066.

3-(2-(4-Methoxy-2-Pyridyl)ethenyl)-N-Confused Tetrakis(*p*-trifluoromethylphenyl)porphyrin Ni(II) Complex (1b-Ni): Compound **5** (60 mg, 0.062 mmol) and ((4-methoxypyridin-2-yl)methyl)triphenylphosphonium chloride (26 mg, 0.062 mmol) were dissolved in 30 mL CH_2Cl_2 and DBU (9.0 µL, 0.061 mmol) was added. The solution was stirred for 15 min in room temperature. After the solvent was removed by evaporation, the residue was separated by silica gel column chromatography with CH_2Cl_2/hexane. The first and third fractions were recrystallized from CH_2Cl_2/hexane to give ***cis*-1b-Ni** and ***trans*-1b-Ni** respectively. Yield: ***cis*-1b-Ni;** 11.3 mg (17%), ***trans*-1b-Ni;** 24.7 mg (37%). ***cis*-1b-Ni**: ^{1}H NMR ($CDCl_3$): δ 3.87 (s, 3H, CH_3), 6.15 (d, J = 13.4 Hz, 1H, olefin), 6.23 (d, J = 13.4 Hz, 1H, olefin), 6.59 (dd, J = 6.0, 2.3 Hz, 1H, Py), 6.78 (d, J = 5.8 Hz, 1H, Py), 6.82 (d, J = 2.1 Hz, 1H, Py), 7.61 (d, J = 4.8 Hz, 1H, β-H), 7.67 (d, J = 5.7 Hz, 1H, β-H), 7.77 (d, J = 5.7 Hz, 1H, β-H), 7.79 (d, J = 4.8 Hz, 1H, β-H), 7.80 (s, 2H, β-H), 7.84 (d, J = 7.6 Hz, 2H, m-ArH), 7.85 (d, J = 8.4 Hz, 2H, m-ArH), 7.87 (d, J = 7.6 Hz, 2H, m-ArH), 7.92 (d, J = 7.6 Hz, 2H, o-ArH), 7.94 (d, J = 8.4 Hz, 2H, o-ArH), 7.96 (d, J = 7.6 Hz, 2H, o-ArH), 7.97 (d, J = 7.9 Hz, 2H, m-ArH), 8.15 (d, J = 7.9 Hz, 2H, o-ArH), 17.3 (br s, 1H, outer NH); ^{13}C NMR ($CDCl_3$, 75 MHz): δ 55.5, 109.2, 113.1, 116.0, 117.1, 121.2, 121.8, 122.0, 122.49, 122.58, 122.62, 122.88, 122.92, 123.94, 123.98, 124.07, 124.1, 124.2, 124.3, 124.35, 124.39, 124.44, 126.05, 126.09, 126.18, 126.22, 127.6, 129.0, 129.19, 129.21, 129.5, 129.6, 129.9, 130.0, 130.4, 130.9, 131.0, 131.3, 132.2, 132.4, 133.2, 133.7, 134.0, 143.3, 144.9, 145.0, 145.5, 146.2, 148.0, 149.1, 151.3, 152.6, 152.9, 154.3, 166.9; ^{19}F NMR ($CDCl_3$, 270 MHz): δ –60.37 (s, 3F, CF_3), –60.42 (s, 6F, CF_3), –60.61 (s, 3F, CF_3); UV-vis (CH_2Cl_2, λ_{max} (nm)) 886 (2020), 797 (2510), 615 (17300), 491 (29200), 455 (30600), 390 (29600); HRMS (ESI-TOF) m/z: $[M]^+$ Calcd for $C_{56}H_{31}F_{12}N_5NiO$ 1075.16905; Found 1075.16932. ***trans*-1b-Ni**: ^{1}H NMR ($CDCl_3$): δ 3.86 (s, 3H, CH_3), 6.56 (d, J = 1.8 Hz, 1H, Py), 6.72 (dd, J = 1.8, 5.5 Hz, 1H, Py), 6.88 (d, J = 16.5 Hz, 1H, olefin), 7.01 (d, J = 16.5 Hz, 1H, olefin), 7.59 (d, J = 4.9 Hz, 1H, β-H), 7.67 (d, J = 4.9 Hz, 1H, β-H), 7.77 (d, J = 4.9 Hz, 1H, β-H), 7.78 (d, J = 4.9 Hz, 1H, β-H), 7.80 (d, J = 4.9 Hz, 1H, β-H), 7.84 (d, J = 4.9 Hz, 1H, β-H), 7.85–7.98 (m, 14H), 8.03 (d, J = 7.9 Hz, 2H, o-Ar), 8.34 (d, J = 5.5 Hz, 1H, Py), 9.83 (br s, 1H, outer NH); ^{13}C NMR ($CDCl_3$, 75 MHz): δ 54.9, 115.8, 117.06, 117.09, 117.2, 119.4, 121.3, 121.92, 121.94, 121.98, 122.03, 122.05, 122.06, 122.08, 122.10, 122.3, 123.9, 124.50, 124.54, 124.59, 125.5, 125.8, 125.9, 126.0, 128.8, 128.9, 129.1, 129.2, 129.5, 129.6, 129.7, 129.9, 130.1, 131.3, 131.9, 132.1, 132.5, 132.9, 133.1, 133.5, 140.67, 140.69, 140.71, 143.81, 143.85, 143.89, 143.90, 143.92, 144.0, 144.2, 144.3, 144.6, 146.1, 148.0, 149.4, 151.4, 152.6, 153.2; ^{19}F NMR ($CDCl_3$, 270 MHz): δ –60.51 (s, 3F, CF_3), –60.52 (s, 3F, CF_3), –60.63 (s, 3F, CF_3), –60.64 (s, 3F, CF_3); UV-vis (CH_2Cl_2, λ_{max}/nm (ε)): 799 (3550), 602 (26000), 452 (59900), 382 (52300); HRMS (ESI-TOF) m/z: $[M+H]^+$ Calcd for $C_{56}H_{31}F_{12}N_5NiO$ 1076.17419; Found 1076.17687.

3-(2-(2-Pyridyl)ethenyl)-N-Confused Tetrakis(*p*-trifluoromethylphenyl)porphyrin (1a): ***trans*-1a-Ni** (27.6 mg, 0.026 mmol) was dissolved in 20 mL of dichloromethane and methanesulfonic acid (0.1 mL) was added. The solution was stirred for 30 min, and aqueous $NaHCO_3$ solution was added. The reaction mixture was washed with water, and the organic layer was separated. After the solvent was evaporated, the residue was separated by silica gel column chromatography with 1% triethylamine in CH_2C1_2 to afford ***trans*-3H-1a** (22.0 mg, 84%) and ***cis*-2H-1a** (3.5 mg, 13%). ***trans*-3H-1a**: ^{1}H NMR ($CDCl_3$, 300 MHz, ppm): δ –4.78 (s, 1H, inner CH), –2.00 (br s, 2H, inner NH), 6.97 (d, J = 15.3 Hz, 1H, olefin), 7.09 (d, J = 7.6 Hz, 1H, Py), 7.12 (dd, J = 3.4, 7.6 Hz, 1H, Py), 7.58 (ddd, J = 3.4, 7.6, 7.8 Hz, 1H, Py), 7.94 (d, J = 15.3 Hz, 1H, olefin), 8.04 (d, J = 8.3 Hz, 2H, m-ArH), 8.04 (d, J = 8.1 Hz, 2H, m-ArH), 8.11 (d, J = 8.3 Hz, 2H, m-ArH), 8.12 (d, J = 7.2 Hz, 4H, m-ArH), 8.27 (d, J = 8.3 Hz, 2H, o-ArH), 8.30 (d, J = 8.1 Hz, 2H, o-ArH), 8.43 (d, J = 5.8 Hz, 1H, β-H), 8.45 (d, J = 4.9

Hz, 1H, β-H), 8.47 (d, *J* = 5.8 Hz, 1H, β-H), 8.48 (d, *J* = 7.2 Hz, 2H, *o*-ArH), 8.50 (d, *J* = 3.4 Hz, 1H, Py), 8.51 (d, *J* = 5.2 Hz, 1H, β-H), 8.54 (d, *J* = 8.3 Hz, 2H, *o*-ArH), 8.84 (d, *J* = 4.9 Hz, 1H, β-H), 8.85 (d, *J* = 5.2 Hz, 1H, β-H); ^{13}C NMR: Because of the isomerization during the measurement, distinct spectrum was unable to obtain; ^{19}F NMR ($CDCl_3$, 270 MHz): δ –60.37 (s, 3F, CF_3), –60.50 (s, 6F, CF_3), –60.61 (s, 3F, CF_3); UV-vis (CH_2Cl_2, λ_{max}/nm (ε)): 765 (10900), 558 (20200), 472 (162000), 374 (53200); HRMS (ESI-TOF) *m/z*: $[M-H]^-$ Calcd for $C_{55}H_{31}F_{12}N_5$ 988.23096; Found 988.23060. ***cis*-2H-1a**: ^{1}H NMR ($CDCl_3$): δ 1.60 (s, 1H, inner CH), 4.09 (br s, 1H, inner NH), 6.02 (d, *J* = 13.6 Hz, 1H, olefin), 6.20 (d, *J* = 13.6 Hz, 1H, olefin), 6.90 (d, *J* = 4.9 Hz, 1H, Py), 7.03 (dd, *J* = 7.0, 5.2 Hz, 1H, Py), 7.25 (d, *J* = 8.9 Hz, 1H, Py), 7.40 (d, *J* = 4.2 Hz, 1H, β-H), 7.46 (d, *J* = 4.2 Hz, 1H, β-H), 7.68 (t, *J* = 8.2 Hz, 1H, Py), 7.68 (s, 2H, β-H),7.78 (d, *J* = 4.2 Hz, 1H, β-H), 7.85 (d, *J* = 4.2 Hz, 1H, β-H), 7.86 (d, *J* = 8.3 Hz, 4H, *m*-ArH), 7.91 (d, *J* = 7.3 Hz, 2H, *m*-ArH), 7.96 (d, *J* = 8.3 Hz, 4H, *o*-ArH), 8.02 (d, *J* = 8.3 Hz, 2H, *m*-ArH), 8.08 (d, *J* = 7.3 Hz, 2H, *o*-ArH), 8.26 (d, *J* = 8.3 Hz, 2H, *o*-ArH), 16.5 (br s, 1H, outer NH); ^{13}C NMR: Because of the isomerization during the measurement, distinct spectrum was unable to obtain; ^{19}F NMR ($CDCl_3$, 270 MHz): δ –60.39 (s, 3F, CF_3), –60.52 (s, 6F, CF_3), –60.72 (s, 3F, CF_3); UV-vis (CH_2Cl_2, λ_{max}/nm (ε)): 742 (16400), 664 (23200), 664 (32200), 614 (17300), 497 (154000); HRMS (ESI-TOF) *m/z*: $[M+H]^+$ Calcd for $C_{55}H_{31}F_{12}N_5$: 990.24661; Found 990.24663.

3-(2-(4-Methoxy-2-Pyridyl)ethenyl)-N-Confused Tetrakis(*p*-trifluoromethylphenyl)porphyrin (1b): *trans*-1b-Ni (29.6 mg, 0.027 mmol) was dissolved in 10 mL of dichloromethane and methanesulfonic acid (0.1 mL) was added. The solution was stirred for 20 min and aqueous $NaHCO_3$ solution was added. The reaction mixture was washed with water and the organic layer was separated. After the solvent was removed by evaporation, the residue was separated by silica gel column chromatography with 1% triethylamine in CH_2Cl_2 to afford ***trans*-3H-1b** (18.0 mg, 64%) and ***cis*-2H-1b** (9.4 mg, 33%). ***trans*-3H-1b**: ^{1}H NMR ($CDCl_3$, 300 MHz, ppm): δ –4.77 (s, 1H, inner CH), –1.99 (br s, 2H, inner NH), 3.85 (s, 3H, OCH_3), 6.65–6.67 (m, 2H, Py), 7.04 (d, *J* = 15.5 Hz, 1H, olefin), 7.86 (d, *J* = 15.5 Hz, 1H, olefin), 8.04 (d, *J* = 6.6 Hz, 4H, *m*-ArH), 8.11 (d, *J* = 7.8 Hz, 4H, *m*-ArH), 8.27 (d, *J* = 7.4 Hz, 2H, *o*-ArH), 8.29 (d, *J* = 7.4 Hz, 2H, *o*-ArH), 8.31 (d, *J* = 6.0 Hz, 1H, Py), 8.47 (d, *J* = 7.8 Hz, 2H, *o*-ArH), 8.55 (d, *J* = 7.8 Hz, 2H, *o*-ArH), 8.42 (d, *J* = 4.9 Hz, 1H, β-H), 8.45 (d, *J* = 5.1 Hz, 1H, β-H), 8.46 (d, *J* = 6.0 Hz, 1H, β-H), 8.50 (d, *J* = 4.9 Hz, 1H, β-H), 8.84 (d, *J* = 4.9 Hz, 2H, β-H); ^{13}C NMR: Because of the isomerization during the measurement, distinct spectrum was unable to obtain; ^{19}F NMR ($CDCl_3$, 270 MHz): δ –60.41 (s, 3F, CF_3), –60.54 (s, 6F, CF_3), –60.65 (s, 3F, CF_3); UV-vis (CH_2Cl_2, λ_{max}/nm (ε)): 765 (5880), 558 (13500), 472 (138000), 379 (43100); HRMS (ESI-TOF) *m/z*: $[M+H]^+$ Calcd for $C_{56}H_{33}F_{12}N_5O$ 1020.25717; Found 1020.25707. ***cis*-2H-1b**: ^{1}H NMR ($CDCl_3$): δ 1.56 (s, 1H, inner CH, 3.99 (br s, 1H, inner NH), 3.84 (s, 3H, CH_3), 6.00 (d, *J* = 13.4 Hz, 1H, olefin), 6.13 (d, *J* = 13.4 Hz, 1H, olefin), 6.54 (dd, *J* = 6.0, 2.0 Hz, 1H, Py), 6.72–6.74 (m, 2H, Py), 7.41 (d, *J* = 4.9 Hz, 1H, β-H), 7.47 (d, *J* = 4.6 Hz, 1H, β-H), 7.69 (br s, 2H, β-H), 7.78 (d, *J* = 4.9 Hz, 1H, β-H), 7.86 (d, *J* = 4.9 Hz, 1H, β-H), 7.86 (d, *J* = 8.2 Hz, 4H, *m*-Ar), 7.91 (d, *J* = 8.1 Hz, 2H, *m*-Ar), 7.96 (d, *J* = 8.2 Hz, 4H, *o*-Ar), 8.02 (d, *J* = 8.1 Hz, 2H *m*-Ar), 8.08 (d, *J* = 8.1 Hz, 2H *o*-Ar), 8.26 (d, *J* = 8.1 Hz, 2H *o*-Ar), 16.82 (br s, 1H, outer NH); ^{13}C NMR: Because of the isomerization during the measurement, distinct spectrum was unable to obtain; ^{19}F NMR ($CDCl_3$, 270 MHz): δ –60.38 (s, 3F, CF_3), –60.52 (s, 6F, CF_3), –60.67 (s, 3F, CF_3); UV-vis (CH_2Cl_2, λ_{max}/nm (ε)): 740 (12200), 663 (16500), 613 (12000), 495 (113000), 375 (54500); HRMS (ESI-TOF) *m/z*: $[M+H]^+$ Calcd for $AgC_{55}H_{28}AgF_{12}N_5$ 1020.25717; Found 1020.25703.

3-(2-(2-Pyridyl)ethenyl)-N-Confused Tetrakis(*p*-trifluoromethylphenyl)porphyrin Ag(III) Complex (*trans*-1a-Ag): ***trans*-1a** (25.0 mg, 0.025 mmol) was dissolved in 20 mL of CH_2Cl_2 and silver(I) acetate (21.5 mg, 0.125 mmol) was added. The solution was stirred for 2 h, and then the solvent was evaporated. The residue was separated by silica gel column chromatography with 1% methanol in CH_2Cl_2 to afford ***trans*-1a-Ag** (15.7 mg, 57%). ^{1}H NMR ($CDCl_3$, 300 MHz, ppm): δ 7.05 (d, *J* = 15.6 Hz, 1H, olefin), 7.14 (d, *J* = 8.2 Hz, 1H, Py), 7.18 (dd, *J* = 6.0, 7.9 Hz, 1H, Py), 7.19 (dd, *J* = 7.7, 7.7 Hz, 1H, Py), 8.03 (d, *J* = 15.6 Hz, 1H, olefin), 8.02–8.07 (m, 8H, *m*-ArH), 8.14 (d, *J* = 7.7 Hz, 2H, *o*-ArH), 8.24 (d, *J* = 8.2 Hz, 2H, *o*-ArH), 8.27 (d, *J* = 8.1 Hz, 2H, *o*-ArH), 8.37 (d, *J* = 7.9 Hz, 2H, *o*-ArH), 8.52 (d, *J* = 5.0 Hz, 1H, β-H), 8.57 (d, *J* = 5.0 Hz, 1H, β-H), 8.57 (d, *J* = 5.0 Hz, 1H, β-H), 8.60 (s, 1H, Py), 8.62 (d, *J* = 4.5 Hz, 1H, β-H), 8.66 (d, *J* = 5.0 Hz, 1H, β-H), 8.85 (d, *J* = 4.5 Hz, 1H, β-H); ^{13}C NMR ($CDCl_3$, 150 MHz): δ 118.9, 119.8, 120.8, 121.9, 122.6, 123.5, 123.6, 123.79, 123.82, 123.84, 124.2, 124.3, 124.46, 124.48, 124.50, 125.3, 125.4, 125.5, 125.6, 126.1, 127.5, 128.2, 128.5, 128.6, 128.8, 129.15, 129.18, 129.6, 129.81, 129.83, 130.06, 130.09, 130.3, 130.5, 130.6, 130.7, 130.8, 130.9, 131.0, 131.5, 133.3, 134.1, 135.7, 136.2, 137.7, 138.84, 138.86, 138.90, 138.92, 139.1, 139.9, 140.5, 141.5, 143.1, 144.2, 144.9, 149.8, 155.4, 164.5; ^{19}F NMR ($CDCl_3$, 270 MHz): δ –60.36 (s, 3F, CF_3), –60.55 (s, 3F, CF_3), –60.58 (s, 3F, CF_3), –60.59 (s, 3F, CF_3); UV-vis (CH_2Cl_2, λ_{max}/nm (ε)): 581 (6860), 534 (8140), 467 (52800), 387 (19700), 332 (17500); HRMS (ESI-TOF) *m/z*: $[M+H]^+$ Calcd for $C_{55}H_{28}F_{12}N_5Ag$ 1094.12821; Found 1094.12823.

3-(2-(2-Pyridyl)ethenyl)tetraphenylporphyrin (7): Triphenyl[(5,10,15,20-tetraphenylporphyrin-2-yl)methyl]phosphonium chloride[17b] (200 mg, 0.22 mmol) and 2-formylpyridine (46.3 mg, 0.43 mmol) were dissolved in 20 mL CH_2Cl_2 and DBU (100 μL, 0.68 mmol) was added. The reaction mixture was stirred for 10 min at room temperature. After the solvent was removed by evaporation, the residue was separated by silica gel column chromatography with CH_2Cl_2/hexane. The first and third fractions were recrystallized from CH_2Cl_2/hexane to give ***cis*-7** and ***trans*-7**, respectively. Yield: ***cis*-7** 33.0 mg (21%), ***trans*-7** 80.0 mg (52%). ***trans*-7**: ^{1}H NMR ($CDCl_3$, 300 MHz, ppm): δ –2.55 (br s, 2H, inner NH), 7.12–7.18 (m, 2H, Py), 7.21 (d, *J* = 16.2 Hz, 1H, olefin), 7.50 (d, *J* = 16.2 Hz, 1H, olefin), 7.64 (dd, *J* = 7.3, 7.3 Hz, 1H, Py), 7.78–7.81 (m, 12H, *m, p*-Ph), 8.23–8.25 (m, 8H, *m, o*-Ph), 8.58 (d, *J* = 4.6 Hz, 1H, Py), 8.77 (d, *J* = 4.8 Hz, 1H, β-H), 8.82 (d, *J* = 4.8 Hz, 1H, β-H), 8.86 (d, *J* = 4.6 Hz, 4H, β-H), 9.13 (s, 1H, β-H); UV-vis (CH_2Cl_2, λ_{max}/nm (ε)): 657 (1510), 600 (3960), 562 (6050), 524 (11300), 427 (141000); HRMS (ESI-TOF) *m/z*: $[M+H]^+$ Calcd for $C_{51}H_{35}N_5$ 718.29707; Found 718.29739. ***cis*-7**: ^{1}H NMR ($CDCl_3$): δ –2.72 (br s, 2H, inner NH), 6.43 (d, *J* = 12.2 Hz, 1H, olefin), 6.71 (d, *J* = 12.2 Hz, 1H, olefin), 6.97–7.03 (m, 3H, Py), 7.57 (t, *J* = 7.3 Hz, 1H, Py), 7.63–7.68 (m, 3H, *m, p*-Ph), 7.75–7.77 (m, 8H, *m, p*-Ph), 7.98 (d, *J* = 7.0 Hz, 2H, *o*-Ph), 8.08 (d, *J* = 7.0 Hz, 2H, *o*-Ph), 8.20 (d, *J* = 7.5 Hz, 4H, *o*-Ph), 8.52–8.54 (m, 2H,

β-H, Py), 8.76–8.84 (m, 6H, β-H); UV-vis (CH_2Cl_2, λ_{max}/nm (ε)): 651 (2750), 596 (5460), 556 (6740), 520 (17600), 422 (272000); HRMS (ESI-TOF) *m/z*: $[M+H]^+$ Calcd for $C_{51}H_{35}N_5$ 718.29707; Found 718.29709.

X-ray crystallography. 1a-Ni: X-ray analysis was performed on a Rigaku VariMax with RAPID equipped with an imaging plate using CuK_α (multi-layer mirror, monochromated, λ = 1.54187 Å) radiation. The structure was solved by the direct method of SIR2004[25] and refined using the SHELXL-2016/6 program.[26] The positional parameters and thermal parameters of non-hydrogen atoms were refined anisotropically on F^2 by the full-matrix least-squares method. Hydrogen atoms were placed at calculated positions and refined riding on their corresponding carbon atoms. **1a-Ag**: X-ray analysis was performed on a Rigaku Saturn 724 equipped with a CCD detector using MoKα (graphite, monochromated, λ = 0.71069 Å) radiation. The structure was solved by the direct method of SIR92[27] and refined using the SHELXL-2016/6 program. The positional parameters and thermal parameters of non-hydrogen atoms were refined anisotropically on F^2 by the full-matrix least-squares method. Hydrogen atoms were placed at calculated positions and refined riding on their corresponding carbon atoms. PLATON/SQUEEZE[28] was used to correct the data for the presence of the disordered solvent.

Calculation Details: All density functional theory calculations[29] were achieved with a Gaussian09[30] program package. The basis sets implemented in the program were used. The B3LYP[31] density functional method was used with the 6-31G** (for C, H, N, F) and LanL2DZ (for Ni) basis set for structural optimizations. Equilibrium geometries were fully optimized and verified by the frequency calculations, where no imaginary frequency was found.

Saturation Transfer Experiment.[32] The determination of the rate constant for NCTPP tautomerism was performed on a JEOL α-500 spectrometer (operating at 500.00 MHz for ^{1}H) with a spin saturation transfer method. The spin relaxation times were estimated by an inversion recovery method. In this experiment, mainly we used the signal of the inner CH. The tautomerism kinetics are shown, where [**3H**] and [**3H***] are the lower and upper spin-state populations for the inner CH of tautomer-**3H**, and [**2H**] and [**2H***] are those for the inner CH of tautomer-**2H**, respectively. $T_{1\,3H}$ and $T_{1\,2H}$ are the spin lattice relaxation times for the inner CH of **2-3H** and **2-2H**, and k_f, k_b are the rate constants of the tautomerism. Here, the signals of **2-2H** were saturated. With a sufficiently long irradiation of the decoupler r. f. pulse, the spin states of the **2-2H** can be saturated; i.e. [**2H**] = [**2H***]. Over time, the saturated spin population is transferred to the signal of **2-2H** via tautomerism, resulting in partial loss of net magnetization of the P(**3H**) signal from its thermal equilibrium value. Then, k_f were calculated according to the equation below.

$$k_f = \frac{1}{T_{1P(3H)}}\left(\frac{I_0}{I} - 1\right) \qquad (1)$$

I_0 is the signal intensity in the thermal equilibrium, and I is that in saturation.

ASSOCIATED CONTENT

Supporting Information.

^{1}H, ^{13}C, and ^{19}F NMR spectra of compounds (PDF)
UV-vis-NIR and FL spectra of compounds (PDF)
Kinetic data of isomerization (PDF)
Calculation data (PDF)
X-ray crystallographic data for compound ***cis*-1a-Ni** (CIF)
X-ray crystallographic data for compound ***trans*-1b-Ag** (CIF)

AUTHOR INFORMATION

Corresponding Author

* hfuruta@cstf.kyushu-u.ac.jp
ORCID
Hiroyuki Furuta: 0000-0002-3881-8807
Masatoshi Ishida: 0000-0002-1117-2188

Notes

The authors declare no competing financial interest.

ACKNOWLEDGMENTS

The work was supported by the Grant-in-Aid (no. 15K13646 to H.F; 16K05700 and 17H05377 to M.I.) from the Ministry of Education, Culture, Sports, Science and Technology of Japan. The financial support from a bilateral program between JSPS and the National Research Foundation (NRF) of South Africa is also acknowledged. P.K.E thanks to the financial support from the internship program of IIT Gandhinagar and Kyushu University.

REFERENCES

(1) *Molecular Switches*, Feringa, B. L., Ed.; Wiley: Weinheim, **2001**.
(2) (a) Dugave, C.; Demange, L. *Chem. Rev*. **2003**, *103*, 2475–2532. (b) *cis-trans Isomerization in Biochemistry,* Dugave, C., Ed.; Wiley: Weinheim, 2006. (c) Irie, M. *Chem. Rev*. **2000**, *100*, 1685–1716. (d) Irie, M.; Fukaminato, T.; Matsuda, K.; Kobatake, S. *Chem. Rev*. **2014**, *114*, 12174–12277. (e) *Tautomerism: Methods and Theories*, Antonov, L., Ed.; Wiley: Weinheim, 2014. (f) *Tautomerism: Concepts and Applications in Science and Technology*, Antonov, L., Ed.; Wiley: Weinheim, 2016.
(3) (a) Obi, M.; Sakuragi, H.; Arai, T. *Chem. Lett.* **1998**, *27*, 169–170. (b) Lewis, F. D.; Yoon, B. A.; Arai, T.; Iwasaki, T.; Tokumaru, K. *J. Am. Chem. Soc.* **1995**, *117*, 3029–3036. (c) Kurihara, S.; Nishimura, Y.; Arai, T. *Bull. Chem. Soc. Jpn*. **2015**, *88*, 963–965.
(4) (a) Furuta, H.; Asano, T.; Ogawa, T. *J. Am. Chem. Soc.* **1994**, *116*, 767–768. (b) Chmielewski, P. J.; Latos-Grażyński, L.; Rachlewicz, K.; Głowiak, T. *Angew. Chem., Int. Ed. Engl.* **1994**, *33*, 779–781.
(5) (a) Furuta, H.; Ishizuka, T.; Osuka, A.; Dejima, H.; Nakagawa, H.; Ishikawa, Y. *J. Am. Chem. Soc.* **2001**, *123*, 6207–6208. (b) Alemán, E. A.; Rajesh, C. S.; Ziegler, C. J.; Modarelli, D. A. *J. Phys. Chem.* A **2006**, *110*, 8605–8612. (c) Ziegler, C. J.; Erickson, N. R.; Dahlby, M. R.; Nemykin, V. N. *J. Phys. Chem.* A **2013**, *117*, 11499–11508. (d) Shaw, J. L.; McMurry, J. L.; Salehi, P.; Stovall, A. *J. Porphyrin Phthalocyanine*s **2014**, *18*, 231–239. (e) Alemán, E. A.; Jojo, J.; Modarelli, D. A. *J. Org. Chem.* **2015**, *80*, 11031–11038. (f) Marchand, G.; Roy, H.; Mendive-Tapia, D.; Jacquemin, D. *Phys. Chem. Chem. Phys.* **2015**, *17*, 5290–5297. (g) Ou, Z.; Chen, X.; Ye, L.; Xue, S.; Fang, Y.; Jiang, X.; Kadish, K. M. *J. Porphyrin Phthalocyanine*s **2015**, *19*, 251–260.
(6) Maeda, H.; Morimoto, T.; Osuka, A.; Furuta, H. *Chem. Asian J.* **2006**, *1*, 832–844.
(7) (a) Zilbermann, I.; Maimon, E.; Ydgar, R.; Shames, A. I.; Korin, E.; Soifer, L.; Bettelheim A. *Inorg. Chem. Commun.* **2004**, 1238–1241. (b) Chmielewski, P. J.; Latos-Grażyński, L.; Schmidt, I. *Inorg. Chem.* **2000**, *39*, 5475–5482. (c) Furuta, H; Kubo, N.; Maeda, H.; Ishizuka, T.; Osuka, A.; Nanami, H.; Ogawa, T. *Inorg. Chem.* **2000**, *39*, 5424–5425. (d) Furuta, H.; Youfu, K.; Maeda, H.; Osuka, A. *Angew. Chem. Int. Ed.* **2003**, *42*, 2186–2188. (e) Harvey, J. D.; Ziegler, C. J. *Chem. Commun.* **2004**, 1666–1667. (f) Maeda, H.; Ishikawa, Y.; Matsuda, T.; Osuka, A.; Furuta, H. *J. Am. Chem. Soc.* **2003**, *125*, 11822–11823. (g) Furuta, H.; Ogawa, T.; Uwatoko, Y.; Araki, K. *Inorg. Chem.* **1999**, *38*, 2676–2682.

(8) Toganoh, M.; Furuta, H., In *Handbook of Porphyrin Science: With Applications to Chemistry, Physics, Materials Science, Engineering, Biology and Medicine;* Kadish, K. M.; Smith, K. M.; Guilard, R., Eds.; World Scientific: New Jersey, **2010**; Vol. 2, Chapter 10, pp. 295–367.
(9) Toganoh, M.; Furuta, H. *Chem. Commun*. **2012**, *48*, 937–954.
(10) Won, D.-H.; Toganoh, M.; Uno, H.; Furuta, H. *Dalton Trans.* **2009**, 6151–6158.
(11) Morimoto, T.; Uno, H.; Furuta, H. *Angew. Chem. Int. Ed.* **2007**, *46*, 3672–3675.
(12) Yan, J.; Yang, Y.; Ishida, M.; Mori, S.; Zhang, B.; Feng, Y.; Furuta, H. *Chem.–Eur. J. Accepted article:* DOI: 10.1002/chem.201701958.
(13) Sakashita, R.; Ishida, M.; Furuta, H. *J. Phys. Chem. A* **2015**, *119*, 1013–1022.
(14) Geier, G. R. III; Haynes, D. M.; Lindsey, J. S. *Org. Lett.* **1999**, 1, 1455–1458.
(15) A Zn complex of *β*-(4-pyridylethenyl)-tetraphenylporphyrin was synthesized and its *cis-trans* isomerization by the photoirradiation or I_2 oxidation was reported. (a) Burrell, A. K.; Officer, D. L.; Reid, D. C. W.; Wild, K. Y. *Angew. Chem. Int. Ed.* **1998**, *37*, 114–117. (b) Bonfantini, E. E.; Burrell, A. K.; Campbell, W. M.; Crossley, M. J.; Gosper, J. J.; Harding, M. M.; Officer, D. L.; Reid, D. C. *J. Porphyrin Phthalocyanines* **2002**, 6, 708–719.
(16) Krygowski, T. M.; Cyrański, M. K. *Chem. Rev.* **2001**, *101*, 1385–1419.
(17) Toganoh, M.; Takayama, T.; Ritesh, N.; Kimizuka, N.; Furuta, H. *Chem. Lett.* **2011**, *40*, 1021–1023.
(18) (a) Schleyer, P. v. R.; Maerker, C.; Dransfeld, A.; Jiao, H.; Hommes, N. v. E. *J. Am. Chem. Soc.* **1996**, *118*, 6317–6318. (b) Chen, Z.; Wannere, C. S.; Corminboeuf, C.; Puchta, R.; Schleyer, P. v. R. *Chem. Rev.* **2005**, *105*, 3842–3888.
(19) A set of data of activation free energy of NH tautomerism is obtained by the spin saturation transfer method for NCTPP in the mixed solvents of pyridine-d_5/$CDCl_3$.
(20) Medforth, C.J. in *The Porphyrin Handbook*, Kadish, K. M.; Smith, K. M.; Guilard, R., Eds; Academic Press: San Diego, 2000; Vol. 5, 1–80.
(21) Braun, J.; Schlabach, M.; Wehrle, B.; Köcher, M.; Vogel, E.; Limbach, H.-H. *J. Am. Chem. Soc.* **1994**, *116*, 6593–6604.
(22) Toganoh, M.; Furuta, H. *J. Phys. Chem.* **2009**, *113*, 13593–13963.
(23) For **1a-Ni**, $\Delta G_o^{\ddagger}{}_{cis\rightarrow trans}$ = 38.9 kcal/mol was obtained from the calculation (Table S7).
(24) Kwon, J. E.; Park, S. Y. *Adv. Mater.* **2011**, *23*, 3615–3642.
(25) Burla, M. C.; Caliandro, R.; Camalli, M.; Carrozzini, B.; Cascarano, G. L.; De Caro, L.; Giacovazzo, C.; Polidori, G.; Spagna, R. *J. Appl. Cryst.* **2005**, *38*, 381–388.
(26) Sheldrick, G. M. *Acta Cryst.* **2015**, *C71*, 3–8.
(27) Altomare, A.; Cascarano, G.; Giacovazzo, C.; Guagliardi, A. *J. Appl. Cryst.* **1993**, *26,* 343–350.
(28) (a) Spek, A. *J. Appl. Crystallogr.* **2003**, *36*, 7–13. (b) van der Sluis, P.; Spek, A. L. *Acta Crystallogr.* **1990**, *A46*, 194–201.
(29) (a) Hohenberg, P.; Kohn, W. *Phys. Rev.* **1964**, *136*, B864. (b) Kohn, W.; Sham, L. *J. Phys. Rev.* **1965**, *140*, A1133.
(30) Frisch, M. J.; Trucks, G. W.; Schlegel, H. B.; Scuseria, G. E.; Robb, M. A.; Cheeseman, J. R.; Scalmani, G.; Barone, V.; Mennucci, B.; Petersson, G. A.; Nakatsuji, H.; Caricato, M.; Li, X.; Hratchian, H. P; Izmaylov, A. F.; Bloino, J.; Zheng, G.; Sonnenberg, J. L.; Hada, M.; Ehara, M.; Toyota, K.; Fukuda, R.; Hasegawa, J.; Ishida, M.; Nakajima, T.; Honda, Y.; Kitao, O.; Nakai, H.; Vreven, T.; Montgomery, J. A. Jr.; Peralta, J.E.; Ogliaro, F.; Bearpark, M.; Heyd, J. J.; Brothers, E.; Kudin, K. N.; Staroverov, V. N.; Keith, T.; Kobayashi, R.; Normand, J.; Raghavachari, K.; Rendell, A.; Burant, J. C.; Iyengar, S. S.; Tomasi, J.; Cossi, M.; Rega, N.; Millam, J. M.; Klene, M.; Knox, J. E.; Cross, J. B.; Bakken, V.; Adamo, C.; Jaramillo, J.; Gomperts, R.; Stratmann, R. E.; Yazyev, O.; Austin, A. J.; Cammi, R.; Pomelli, C.; Ochterski, J. W.; Martin, R. L.; Morokuma, K.; Zakrzewski, V. G.; Voth, G. A.; Salvador, P.; Dannenberg, J. J.; Dapprich, S.; Daniels, A. D.; Farkas, O.; Foresman, J. B.; Ortiz, J. V.; Cioslowski, J.; Fox, D. J. Gaussian 09, Revision B.01, Gaussian, Inc., Wallingford CT, **2010**.
(31) (a) Becke, A. D. *J. Phys. Chem.* **1993**, *98*, 5648–5652. (b) Lee, C.; Yang, W.; Parr, R. G. *Phys. Rev. B* **1988**, *37*, 785–789. (c) Vosko, S. H.; Wilk, L.; Nusair, M. Can. *J. Phys.* **1980**, *58*, 1200–1211. (d) Stephens, P. J.; Devlin, F. J.; Chabalowski, C. F.; Frisch, M. J. *J. Phys. Chem.* **1994**, *98*, 11623–11627.
(32) Jorek, R. L.; Flesher, R. J.; Shin, S. K. *J. Chem. Educ.* **1997**, *74,* 978–982.

SYNOPSIS TOC

Pyridylethenyl-substituted N-confused porphyrin showed the thermal *cis-trans* isomerization at 30 °C in solution. The kinetics study revealed the activation energy from *cis* to *trans* isomer is lowered significantly to $\Delta G^{\ddagger}_{o\ cis\rightarrow trans}$ = 35.7 kcal/mol. The intermolecular proton transfer induced *cis-trans* isomerization mechanism was proposed.